*Graphical Abstract (for review)

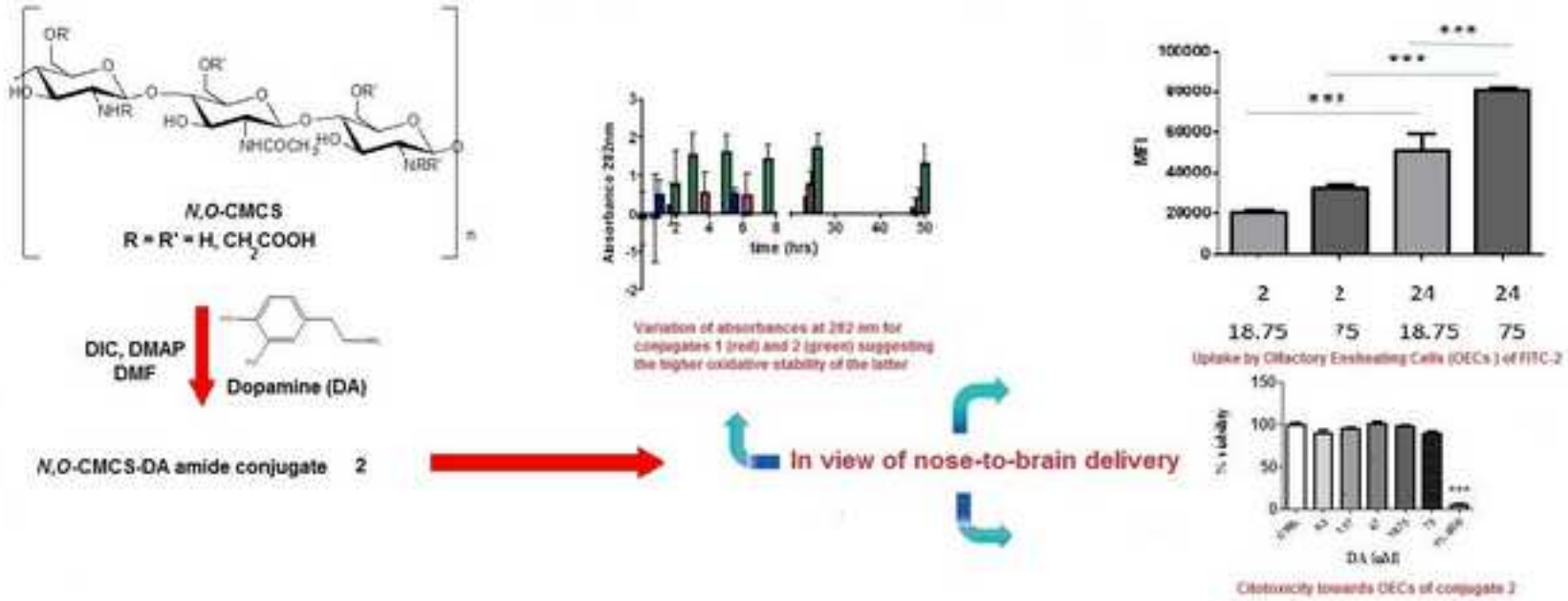

# Nose-to-brain delivery: a comparative study between carboxymethyl chitosan based conjugates of dopamine

Sante Di Gioia[a], Adriana Trapani[b,], Roberta Cassano[c,*], Maria Luisa Di Gioia[c], Sonia Trombino[c] , Saverio Cellamare[b], Isabella Bolognino[b], Md Niamat Hossain[a], Enrico Sanna[d], Giuseppe Trapani[b], Massimo Conese[a]

This work is dedicated to the memory of deceased Prof. Nevio Picci

[a]*Department of Medical and Surgical Sciences, University of Foggia, 71122 Foggia, Italy*

[b]*Department of Pharmacy-Drug Sciences, University of Bari "Aldo Moro", 70125 Bari, Italy*

[c]*Department of Pharmacy, Health and Nutritional Sciences, University of Calabria, 87036 Arcavacata di Rende, Cosenza, Italy*

[d]*Department of Life and Environmental Sciences, Section of Neuroscience and Anthropology, University of Cagliari, Monserrato (Cagliari), Italy*

Corresponding Authors:

*Prof. Adriana Trapani

Department of Pharmacy-Drug Sciences

University of Bari "Aldo Moro", Bari, Italy

Tel.: +39-0805442114. Fax: +39-0805442724.

Email: adriana.trapani@uniba.it

* Prof. Roberta Cassano

Department of Pharmacy,

Health and Nutritional Sciences, Università della Calabria,

Arcavacata di Rende, Cosenza, Italy

Tel:/Fax: +39 984 493203.

E-mail: roberta.cassano@unical.it

**Abstract**

Herein, the synthesis of a novel polymeric conjugate *N,O*-CMCS-Dopamine (DA) based on an amide linkage is reported. The performances of this conjugate were compared with those of an analogous *N,O*-CMCS-DA ester conjugate previously studied (Cassano et al., 2020) to gain insight into their potential utility for Parkinson's disease treatment. The new amide conjugate was synthesized by standard carbodiimide coupling procedure and characterized by FT-IR, $^{1}$H-NMR spectroscopies and thermal analysis (Differential Scanning Calorimetry). *In vitro* mucoadhesive studies in simulated nasal fluid (SNF) evidenced high adhesive effect of both ester and amide conjugates. Results demonstrated that the amide conjugate exerted an important role to prevent DA spontaneous autoxidation both under stressed conditions and physiological mimicking ones. MTT test indicated cytocompatibility of the amide conjugate with Olfactory Ensheating Cells (OECs), which were shown by cytofluorimetry to internalize efficiently the conjugate. Overall, among the two conjugates herein studied, the *N,O*-CMCS-DA amide conjugate seems a promising candidate for improving the delivery of DA by nose-to-brain administration.

***Keywords*:** Polymeric conjugates, Dopamine, Oxidative stability, Mucoadhesion, Cytotoxicity, Uptake by OEC cells.

List of chemical compounds studied in the article: Dopamine hydrochloride (Compound CID: 65340), Chitosan (Compound CID: 129662530), Hydrogen peroxide (Compound CID: 22326046), *N,N'*-diisopropyl-carbodiimide (Compound CID: 12734), 4-dimethylaminopyridine (Compound CID 14284), Sodium Sulphate (Compound CID: 516914), *N,O*-carboxymethyl chitosan–Dopamine amide conjugate, Hydroxyethyl cellulose (Compound CID: 4327536), Potassium Bromide (Compound CID: 253877), Dimethylsulfoxide (Compound CID: 21584481).

## Introduction

Neurodegenerative diseases (NDs) are chronic, progressive debilitating conditions characterized by the loss of neurons and weakening of brain functions whose incidence increases as the population ages and they represent one of the leading medical challenges faced by our society. One of the main obstacles encountered in the treatment of these diseases is the transport of therapeutic agents across the blood-brain barrier (BBB) which, even though more permeable, is still able to protect the brain from molecules that can cause neuronal damage (Saraiva et al., 2016).

Parkinson's disease (PD) is the second most common ND disease in developed countries after Alzheimer's disease (Reeve et al., 2014) and is characterized by the loss of dopaminergic neurons in the Substantia Nigra and decreased dopamine (DA) levels in the striatum. The presence of intracytoplasmic inclusions, known as Lewy bodies, comprised by abnormal aggregates of proteins such as α-synuclein and ubiquitin, is the pathological characteristic of the disease (Conese et al., 2019). The parkinsonian patient shows both motor symptoms such as tremor, rigidity, bradykinesia and postural instability as well as several non-motor signs as gastrointestinal ones (Wollmer and Klein, 2017).

The standard treatment for controlling PD motor symptoms is based on the "dopamine replacement strategy" consisting in the compensation of the loss of dopaminergic neurons and to restore satisfactory levels of the neurotransmitter. However, DA as such is unable to overcome the BBB because of its physicochemical and metabolic characteristics (Di Gioia et al., 2015). Therefore, a precursor of DA is adopted, L-Dopa, which is able to overcome the BBB employing an active transport system (*i.e.*, the L-large neutral amino acid transporter (Wade and Katzman, 1975)) and it is converted in the brain into the neurotransmitter by L-Dopa-decarboxylase enzyme (Hawthorne et al., 2016; Pahuja et al., 2015). Unfortunately, L-Dopa treatment is not disease-modifying, and, at later stages of the disease, it is unable to control PD motor symptoms and adverse effects emerge including dyskinesia.

An attractive approach to bypass the BBB in NDs is constituted by the intranasal delivery of therapeutic agents for which a direct access to the brain can be accomplished exploiting the olfactory or trigeminal connections between the nose and the brain (Agrawal et al., 2018; Bourganis et al., 2018; Conese et al., 2019; Samaridou and Alonso, 2018). This administration route may be even an effective alternative to the oral one which is characterized by patient compliance and the endorsement of pharmaceutical industry (Kaur et al., 2019; Musani and Chandan, 2015; Trapani et al., 2004). To address the drawbacks consequent to the short residence time in the nasal cavity and to the presence of metabolic enzymes in the olfactory mucosa, the use of potent biologically active substances,

permeation enhancers and mucoadhesive delivery systems have been suggested (Agrawal et al., 2018; Bourganis et al., 2018; Conese et al., 2019; Samaridou and Alonso, 2018).

Advances in the nanomedicine field showed that several nanocarriers, when appropriately tailored, are able to improve drug transport across the BBB showing a great potential for the treatment of NDs (Hawthorne et al., 2016; Kreuter, 2014; Patel et al., 2012). Thus, for instance, the synthetic approach based on laser ablation allows the production of nanomaterials with very low size (< 100 nm) and for several applications including the BBB crossing (Ancona et al., 2014; Singh et al., 2020). In the case of PD, in order to restore the DA content, such noninvasive approach has been evaluated by encapsulating in colloidal carriers of natural or synthetic origin both the free neurotransmitter and dopaminergic drugs (De Giglio et al., 2011; Md et al., 2013; Pahuja et al., 2015; Pillay et al., 2009; Rashed et al., 2015; Trapani et al., 2011). A possible pitfall of this approach may be the premature leakage of the cargo and, to limit this drawback, the conjugation of the active principle to a polymeric backbone by a cleavable chemical bond is pursued. These macromolecular conjugates offer the advantage to solve several problems including prolonged circulation, controlled release as well as improved mucoadhesive properties (Ekladious et al., 2019; Mandracchia et al., 2017; Trapani et al., 2014). Moreover, unlike analogous DA conjugates with low molecular weight moieties (Denora et al., 2012; Mandracchia et al., 2018), they may give rise to polymeric nanoparticles, potentially able to cross the BBB, thanks to their potential to enter the brain capillary by means of endocytosis mechanism (Hawthorne et al., 2016; Li et al., 2017). Of course, in such case, the premature leakage and rapid cargo release is hampered by the presence of the chemical bond between the active principle and the polymer backbone.

In this context, we have recently reported the synthesis and characterization of novel carboxylated chitosan-dopamine conjugates and assessed their *in vitro* mucoadhesive properties in simulated nasal fluid, toxicity and internalization by Olfactory Ensheathing Cells (OECs) for potential nose-to-brain delivery of the neurotransmitter (Cassano et al., 2020). More specifically, we designed the synthesis of some *N,O*-carboxymethyl chitosan-dopamine (*N,O*-CMCS-DA) conjugates characterized by an ester function between the –COOH and the -OH groups of the chitosan derivative and the neurotransmitter, respectively. The cytotoxicity of these conjugates on OECs resulted negligible and, interestingly, their uptake by OECs resulted efficient. Among the conjugates evaluated, the *N,O*-CMCS-DA ester conjugate **1** (Figure 1) seemed promising for improving the delivery of DA by nose-to-brain administration.

**[**Insert Figure 1]

As a continuation of the previous work, in the present paper we report the synthesis and the biological evaluation of the corresponding amide conjugate **2** (Figure 1) resulting from the conjugation of the -

$NH_2$ group of the neurotransmitter with the –COOH function of the *N,O*-CMCS polymer. It was synthetized with the aim to evaluate its potential for nose-to-brain administration in comparison with that observed for the ester conjugate **1**. Besides the synthesis of conjugate **2**, herein we describe the evaluation of its mucoadhesive properties, DA release kinetics as well as the cytotoxicity towards OECs and uptake by such cell type. Moreover, taking into account that a peculiar feature of DA is its possible autoxidation reaction to give products such as reactive oxygen species (ROS) which can damage cellular components and may be involved in PD pathogenesis (Conese et al., 2019; Trapani et al., 2018), the oxidative stability of conjugates **1** and **2** was also assessed.

## 2. Materials and methods

### *2.1. Materials*

*N,O*-Carboxymethyl Chitosan (*N,O*-CMCS, Molecular weight in the range of 30-500 kDa, deacetylation degree, 94.2%; viscosity 22 mPa sec) was purchased from Heppe Medical Chitosan GmbH (Halle, Germany). *N,N'*-diisopropyl-carbodiimide (DIC), 4-dimethylaminopyridine (DMAP), anhydrous *N,N*-dimethylformamide (DMF), dimethylsulfoxide (DMSO), dopamine hydrochloride (DA), porcine stomach mucin (type II, bound sialic acid ~1%), fluorescein 5(6)- isothiocyanate (FITC), ethyl acetate, sodium sulphate and PBS were purchased from Sigma-Aldrich (Milan, Italy). Hydroxyethyl cellulose (HEC, Natrosol 250) was provided by Aakon Polichimica (Milan, Italy). The viscosity of a solution of HEC (2% concentration in water) was equal to 5500 mPa sec (as reported in the manufacturer's instructions). Hydrogen peroxide (3%, Italian Pharmacopeia, 10 volumes stabilized) was purchased from a local pharmacy. Foetal Bovine Serum (FBS) was provided by Corning Life Sciences (Tewksbury, MA, USA). Dialysis tubes with a MWCO 12-14 kDa were purchased from Spectra Labs (Milan, Italy). Throughout this work, double distilled water was used. All other chemicals used were of reagent grade.

### *2.2. Apparatus*

The conjugate **2** was prepared according to the synthetic procedure outlined in Scheme 1 and it was characterized by Fourier transform infrared (FT-IR)- and Proton nuclear magnetic resonance ($^1$H NMR)-spectroscopy as well as by differential scanning calorimetry (DSC). FT-IR spectra were obtained in KBr discs using a Perkin Elmer 1600 FT-IR spectrometer (Perkin Elmer, Italy). The range examined was 4,000–400 $cm^{-1}$ with a resolution of 1 $cm^{-1}$. $^1$H NMR spectra were recorded on a Brüker spectrometer operating at 300 MHz. The analyses were performed at 293 °K on dilute solutions of each compound using $DMSOd_6$ as solvent. Chemical shifts are reported in δ units (ppm) with TMS as reference (δ 0.00). All coupling constants (J) are reported in Hertz. Multiplicity is

indicated by one or more of the following: s (singlet), d (doublet), t (triplet), q (quartet), m (multiplet). DSC thermograms were obtained using a Mettler Toledo DSC 822e STARe 202 System equipped with a DSC MettlerSTARe Software. For DSC analysis, aliquots of about 5 mg of each product were placed in an aluminium pan and hermetically sealed. The scanning rate was of 5 °C/min under a nitrogen flow of 20 $cm^3$/min and the temperature range was from 25 to 275 °C and 25 to 300 °C for *N,O*-CMCS and amide conjugate **2** and DA, respectively. The calorimetric system was calibrated using indium (purity 99.9%) and following the procedure of the MettlerSTARe Software. Each experiment was carried out in triplicate.

*2.3. Synthesis of N,O-Carboxymethyl Chitosan-DA amide conjugate **2***

To a solution of *N,O*-CMCS (0.2 g) in DMF (5 mL), DMAP (0.33 g, 2.74 x $10^{-3}$ mol) and DIC (0.28 mL, 1.82 x $10^{-3}$ mol) were added and the mixture was left at room temperature (r.t.) under magnetic stirring for 10 minutes. Then, dopamine hydrochloride (DA) (0.28 g, 1.82 x $10^{-3}$ mol) was added and the mixture was left at r.t. under stirring overnight. Afterwards, the solvent was evaporated under vacuum and the residue was extracted with ethyl acetate. The combined extracts were washed several times with water, dried over sodium sulfate, filtered and finally evaporated under reduced pressure conditions. The obtained product (*N,O*-Carboxymethyl Chitosan-DA amide conjugate **2**) was collected in good yield (about 70%) and characterized by FT-IR, $^1$H NMR and DSC. *N,O*-CMCS-DA amide conjugate **2**: FT-IR (KBr) ν ($cm^{-1}$): 3541-3236 (NH, OH), 3124, 3028 (CH aromatic), 2933, 2926 (CH aliphatic), 1640, 1619 (C=O), 1114, 1069 (OH). $^1$H-NMR (DMSO-$d_6$) δ (ppm): 9.00 (br s, OH-DA), 6.86 (s, 1 H aromatic DA), 6.70-6.48 (m, 2H aromatic DA), 4.12 (m, 1H anomeric), 3.60-3.50 (m, 5H OCH2CONHR and glucopyranose ring CH), 3.40-3.37 (m, 2H, –O-$\underline{CH_2}$-CONH), 3.15 (m, 1H, Ar-$CH_2$-$\underline{CH_2}$NHCHC=O), 2.90-2.84 (m, 2H, Ar-$\underline{CH_2}$-$CH_2$NHCHC=O ), 1.86 (m, 1H, Ar-$CH_2$-$\underline{CH_2}$NHCHC=O).

*2.3.1. Determination of substitution degree (DS) of conjugate **2***

The substitution degree (DS) of *N,O*-CMCS-DA amide conjugate **2** was calculated following the procedure previously reported for ester conjugates (Cassano et al., 2020). Briefly, suitable amounts of sample were weighted (50 mg) and dissolved in a solution of NaOH (0.25 M) in ethanol (5 mL) and the mixture was kept under stirring at 100 °C for 24 h. Then, a titration with HCl (0.1 N) was made using phenolphthalein as pH indicator for the first equivalence point and the methyl red for the second one. The first point is equivalent headline in excess of soda V2 equivalent point; the second equivalent point indicates the neutralization of the acid salt present V1 equivalent point. The moles

of hydrochloric acid between the first and the second equivalent point corresponding to the moles of free amide and the DS is, therefore, determined by the following Equation:

$$DS = \frac{\text{MM glucose unit}}{(\text{g sample}/\text{ n free amide} - \text{MM free amide} - \text{MM } H_2O)}$$

where n free amide is equal to (V2 equivalent point - V1 equivalent point)·[HCl]; MM glucose unit is the molecular mass of glucose unit; g sample the weight of sample; n free amide the mol of free amide; MM free amide the molecular mass of free amide and MM $H_2O$ the molecular mass of water.

*2.4. Quantitative determination of dopamine*

The quantitative determination of DA was carried out by HPLC as previously reported (Cassano et al., 2020) with slight modifications in order to improve the resolution of HPLC peaks. In details, the composition of the mobile phase consisted of 0.02 M potassium phosphate buffer, pH 2.8: $CH_3OH$ 70:30 (v/v), and the elution of the column in isocratic mode took place at the flow rate of 0.7 mL/min. Under such chromatographic conditions, retention time of DA was equal to 5.5 min, whereas retention time of both conjugates 1 and 2 were equal to 4.9 min.

*2.5. In vitro evaluation of mucoadhesive properties of amide conjugate **2** and the parent polymer N,O-CMCS*

The mucoadhesive properties of *N,O*-CMCS and amide conjugate **2** were evaluated in Simulated Nasal Fluid (SNF) by using an *in vitro* method based on turbidimetric measurements as already described for the ester conjugate **1** (Trapani et al., 2014). SNF consisted of an aqueous solution containing $CaCl_2$ $2H_2O$ (0.32 mg/mL), KCl (1.29 mg/mL) and NaCl (7.45 mg/mL) at pH 6.0 (Pagar et al., 2014). Briefly, freshly prepared mucin dispersions in SNF (0.5 mg/mL) were kept at 37 °C under stirring (150 rpm) for 24 h before to start with the experiment. Then, both amide conjugate **2** and parent polymer *N,O*-CMCS **1** were dispersed in a mixture of SNF/DMSO 0.05% (v/v) to give the final concentration of 0.04% (w/v). To a mucin dispersion in SNF (6 mL) a dispersion of conjugate (or parent polymer) (6 mL) was added and the turbidity of the corresponding mixtures maintained at 37 °C and under stirring (150 rpm) was determined at 650 nm wavelength using a Perkin-Elmer Lambda Bio 20 spectrophotometer at different time points (*i.e.*, 0, 2, 5, 7 and 24 h). HEC dissolved in SNF containing 0.05% (v/v) of DMSO at the concentration of 0.4 mg/mL was employed as positive control. All experiments were carried out in triplicate.

*2.6. In vitro release studies*

*2.6.1. Release of dopamine from ester conjugate **1** and amide conjugate **2** in Simulated Nasal Fluid (SNF)*

The DA release in SNF from ester **1** or amide **2** conjugates was evaluated as follows: a weighted amount of conjugate corresponding to 1-1.2 mg of DA was dispersed in SNF (1.5 mL) containing 0.05% (v/v) of DMSO as dispersing agent without enzymes and thermostated at 37 ± 0.1°C in an agitated (40 rpm/min) water bath (Julabo, Milan, Italy). At scheduled time points, 0.2 mL of the receiving medium were withdrawn and replaced with 0.2 mL of fresh medium (Cassano et al., 2020). Then, each sample was centrifuged at 16,000 × g for 45 min, (Eppendorf 5415D, Germany), and the amounts of the neurotransmitter formed were determined in the resulting supernatants by HPLC, as above described, and plotted against the time. All the release experiments in SNF were carried out in triplicate.

*2.6.2. Determination of dopamine release kinetic from ester **1** and amide **2** conjugates in Fetal Bovine Serum (FBS)*

The DA release in FBS from ester and amide conjugates (**1** and **2**, respectively) was studied as follows. Firstly, 20 mg of conjugate (**1** or **2**) were dispersed in 750 μL of DMSO:PBS 0.05 M pH 7.4 (1:20 v:v) under sonication (Branson 1510, Fisher Scientific, Milan, Italy) for 20 min. Then, the resulting mixture was added to 750 μL of preheated FBS solution and it was maintained in a thermostatic water bath (Julabo, Milan, Italy) at 37 °C. At appropriate time points, aliquots of 100 μL were withdrawn and added to 900 μL of cold acetonitrile in order to deproteinize the serum. After mixing and centrifugation (16,000×g, 45 min, Eppendorf 5415D, Germany), the resulting clear supernatant was diluted 1:1 with 0.02 M potassium phosphate buffer (pH 2.8) and the amounts of the neurotransmitter formed were determined in the resulting supernatants by HPLC as above described. Such amounts were plotted against the square root of the time from which the corresponding Higuchi parameters were derived. All the stability experiments in FBS were carried out in triplicate.

*2.7. Protection from oxidation of N,O-Carboxymethyl Chitosan amide (**1**) ester **1** and N,O-Carboxymethyl Chitosan amide conjugate **2***

The oxidative stability of the ester conjugate **1** and amide conjugate **2** was studied using UV-Vis Spectrophotometric methods (quartz cuvettes, final volume 3mL). Three different experimental conditions were explored*: i)*in cuvettes for spectrophotometry (final volume 3 mL) under three different experimental conditions*: i)* Oxidation upon stressed conditions consisting in a solution of each conjugate in a mixture of hydrogen peroxide:DMSO:water in 1:3:6 volume ratio, respectively

and continuous air bubbling (P = 1 bar) (Trapani et al., 2018). At predetermined time points (0, 1, 3, 6, 17, 24 h) aliquots of 0.2 mL were withdrawn and freeze dried for 72 h (Lio Pascal 5P, Milan, Italy). Afterwards, the resulting powders were re-dissolved in double distilled water and the study was followed by UV-Vis spectrophotometry (Agilent/HP 8453 UV-Vis Spectrophotometer-Spectroscopy System) monitoring the absorbance at 450 nm attributable to aminochrome (AC) (Bisaglia et al., 2007). *ii)* Oxidation upon stressed conditions consisting in air bubbling for 1 min into a mixture of conjugates **1** and **2** or DA or *N,O*-CMCS in a solution of hydrogen peroxide (3%, v/v, 0.52 mL) and recording the corresponding UV spectra at 282 nm (attributable to pure DA) at scheduled time points as well as on a final withdrawal performed at 48 h. The air used was at P = 1 bar and filtered with a 0.45 μm filter (Levanchimica, Bari, Italy) and all the experiments were carried out at 25 °C under magnetic stirring for each cuvette in a thermostatic water bath (Heraeus Thermo Scientific B15 compact incubator). Importantly, no freeze-drying treatment was adopted in this set of experiments. *iii)* Oxidation in the absence of both hydrogen peroxide and DMSO. In this set of experiments, pure DA, conjugate **2**, and pure *N,O*-CMCS were each incubated at the concentration of $10^{-3}$ M for 24 h in PBS (100 mM-pH 7.7) after an initial air bubbling for 5 min and in the absence of both hydrogen peroxide and DMSO. UV spectra were acquired at the wavelengths of 386 and 450 nm at scheduled time points within 40 h (Klegeris et al., 1995).

### *2.8. Preparation of and FITC-N,O-carboxymethyl chitosan-DA amide conjugate **2***

To evaluate the cellular uptake, *N,O*-carboxymethyl chitosan-DA conjugate **2** was labelled with fluoresceine isothiocyanate (FITC) by using a previously reported protocol with slight modifications (Di Gioia et al., 2015). Briefly, *N,O*-carboxymethyl chitosan-DA amide conjugate **2**, (100 mg) was dissolved in 1 N HCl (12 mL) and then the pH was adjusted to 6.5 with 0.1 N NaOH (1 mL). FITC was dissolved at 20 mg/mL concentration in ethanol and 0.75 mL of this solution were added to amide conjugate **2** dispersion, under magnetic stirring at r.t. for 24 h under light protection. Afterwards, the mixture was dialyzed against double distilled water for 3 days and freeze-dried for 72 h (Lio Pascal 5P). The labelling efficiency of FITC-*N,O*-CMCS DA amide conjugate **2** was determined calibrating the fluorometer (Perkin Elmer, Italy) in the range 1-140 ng/mL of FITC prepared by diluting 100 μg/mL of a methanol solution of FITC with phosphate buffer at pH 8.0 (excitation wavelength: 488 nm; emission wavelength: 525 nm; slits: 2.5 nm). Labelling efficiency of the amide conjugate **2** was calculated as percentage of mass FITC/mass FITC-amide conjugate **2**.

### *2.9. Cytotoxicity of amide conjugate **2** against Olfactory Ensheathing Cells (OECs)*

OECs were obtained from 2-day-old mouse pups as previously described (Cassano et al., 2020; Musumeci et al., 2014). OECs were plated at the number of 30,000 per each well of a 96-well plate and, on the following day, were incubated with CMCS-DA conjugate **2** (in a range between 0.3 and 75 μM) in complete medium (DMEM/FBS supplemented with a bovine pituitary extract). Cells were then tested for viability after 24 h by the 3-(4,5-dimethylthiazol-2-yl)-2,5 diphenyl tetrazolium bromide (MTT) assay, as previously described (Di Gioia et al., 2015). The relative viability was calculated in respect to control untreated cells (considered as 100%). 0.1% DMSO (v/v) was used as dispersing agent and internal control for excipient, while 10% Triton-X-100-treated cells were used as positive control.

*2.10. Uptake of amide conjugate **2** by OECs*

OECs (plated at the number of 50,000 per each well of a 24-well plate) were incubated with either FITC-DA-CMCS conjugate **2** in complete medium and in order to obtain the final concentrations of 18.75 and 75 μM. After 2 or 24 h, each well was treated with 0.04% trypan blue in PBS (in order to quench extracellular fluorescence), trypsinized, resuspended in 0.5 mL of PBS, and by Amnis Flowsight IS100 (Merck). Brightfield scatter plots obtained by plotting Area on x-axis vs Aspect Ratio on y-axis were generated, then single cells events were gated, and finally 10,000 single-cell events for sample were acquired. The percentage of green positive cells (channel 2, 488 nm excitation laser) and mean fluorescence were analysed using Amnis IDEAS software (Castellani et al., 2018).

*2.11. Statistics*

Statistical analyses were carried out by Prism v. 4, GraphPad Software Inc., USA. Data were expressed as either mean ± SD or SEM. Multiple comparisons were based on one-way analysis of variance (ANOVA) with the either Bonferroni's or Tukey's post hoc test and differences were considered significant when $p < 0.05$.

## 3. Results

*3.1. Synthesis of the amide conjugate **2***

As shown in Scheme 1, DIC mediated coupling reaction between *N,O*-CMCS polymer and DA was employed to prepare the required *N,O,*-CMCS-DA amide conjugate **2** in the presence of DMAP and in DMF as solvent. The conjugate **2** was structurally characterized on the basis of FT-IR and $^{1}$H-NMR spectroscopic analyses (see section 2.3) as well as by differential scanning calorimetry (DSC). As shown in Figure S1, in the FT-IR spectrum a characteristic absorption bands at 1640 $cm^{-1}$ and

1619 $cm^{-1}$ were present, attributable to the carbonyl groups of **2**. In this regard, it should be noted that, in the FT-IR spectrum of *N,O*-CMCS we used, no absorption band at 1730 $cm^{-1}$ occurs suggesting that it is in the –COONa form (Mourya et al., 2010; Perteghella et al., 2020). Moreover, in the corresponding $^{1}$H-NMR spectrum, the characteristic signals attributable to the protons in *orto* and *meta* positions of the aromatic ring of DA were detected in the range 6.86-6.48 ppm (Figure 2).

[Insert Scheme 1]

Information on the solid state of the amide conjugate **2** was obtained comparing its DSC thermogram with those of pure starting polymer *N,O*-CMCS and pure DA (Figure S1). The thermogram of the neurotransmitter revealed an endothermic peak at 250 °C corresponding to the melting of the neurotransmitter, whereas the thermogram of pure *N,O*-CMCS showed an endothermic peak at 150 °C which, following literature suggestions, should be due to water evaporation (Mourya et al., 2010). The thermogram of the amide conjugate **2** was similar to that of the parent polymer except for the presence of a weak endothermic peak at higher temperature (172 °C). Similarly to that observed for pure *N,O*-CMCS, the glass transition temperature (Tg) was not observed in the thermogram of amide conjugate **2**, even though it seems a pattern suggesting a large amount of amorphous state (Mourya et al., 2010). Probably, it can be accounted for assuming that the Tg of amide conjugate **2** occurs at high temperature where its assessment is prevented by the degradation of this conjugate (Mourya et al., 2010). This interpretation was fully confirmed by recording the DSC thermogram up to 310 °C and, under such conditions, an exothermic peak at 283°C was detected attributable to conjugate **2** decomposition. The DS of amide conjugate **2** was determined by acid-base volumetric titration employing two pH indicators (Section 2.3.1.) using an excess of ethanol solution of NaOH to hydrolyze the amide conjugate. The excess of NaOH was determined by a titration with HCl employing phenolphthalein as pH indicator, while methyl red was used to evidence the neutralization of the acid salt present (Bukzem et al., 2016; Cassano et al., 2007). The measured DS value of amide conjugate **2** was 560 μg of DA/ mg of amide conjugate.

[Insert Figure 2]

*3.2. In vitro evaluation of mucoadhesive properties of amide conjugate **2***

The mucoadhesive properties of amide conjugate **2** and its parent polymer were determined *in vitro* by turbidimetric measurements (Cassano et al., 2020) in a medium consisting of SNF containing little amount of DMSO [0.05% (v/v)] to allow the complete solubilisation of **2**. For sake of comparison,

the previously studied ester conjugate **1** was also included in this study. Due to the fact that Carbopol 940 precipitated in SNF, HEC was herein included as positive control, being endowed with good mucoadhesive features (Ivarsson and Wahlgren, 2012). As shown in Figure 3, essentially the amide conjugate **2** resembled the behavior of ester conjugate **1** in terms of mucoadhesion, whereas the unconjugated *N,O*-Carboxymethyl Chitosan provided the highest decrease of transmittance values only at the initial time points. Indeed, as already seen for ester conjugate **1** (Cassano et al., 2020), a distinct reduction in transmittance value was observed after 24 h of incubation for amide conjugate **2**, which resulted in a statistically very significant difference ($p < 0.01$) *vs* HEC. On the other hand, the differences in transmittance decrease between parent *N,O*-CMCS and HEC were not significant. It is to be pointed out that in the course of these mucoadhesion studies referred to the amide conjugate **2**, no colour change at any time of incubation was detected, while, for ester conjugate **1** after 24 h of incubation it was observed, probably due to the autoxidation process of the neurotransmitter released by hydrolytic cleavage in SNF of this ester conjugate (Ivarsson and Wahlgren, 2012).

Hence, based on these turbidimetric measurements, the mucoadhesive properties of the tested materials can be classified in the following rank order: *N,O*-CMCS-DA ester **1** $\underline{\sim}$ *N,O*-CMCS-DA amide **2** > *N,O*-CMCS ~ HEC.

[Insert Figure 3]

*3.3. Release studies of neurotransmitter from ester **1** and amide **2** conjugates in Simulated Nasal Fluid (SNF) and in Foetal Bovine Serum (FBS)*

The amide **2** and ester **1** conjugates were evaluated by the HPLC method reported in Section 2.4 to assess whether they can be hydrolyzed to give the neurotransmitter in SNF (pH 6.0 without enzymes) and the corresponding results are shown in Figure 4a and 4b, respectively. While after 3 h only about 15% of DA was released from conjugate **1** as earlier reported (Cassano et al., 2020), the neurotransmitter release from the amide **2** was much slower and only after ten days resulted of about 12% (Figure 4a and 4b). Moreover, it should be considered that under the conditions used (pH 6.0 without enzymes) further degradation products of neurotransmitter are negligible (Umek et al., 2018). The decomposition of *N,O*-CMCS-DA conjugates **1** and **2** in FBS [DMSO:PBS 0.05 M pH 7.4 (1:20 v:v)] **1** and **2** may be followed measuring the amount of neurotransmitter released *via* chemical or enzymatic cleavage. However, it should be taken into account that free DA, unlike bound DA, is unstable and slowly gives rise to further degradation products. The kinetics of these consecutive reactions involving DA release from corresponding macromolecular conjugates may be evaluated following the approach reported in literature for

(poly)aspartamide-DA conjugates (Juriga et al., 2018). Briefly, in this work the kinetics of macromolecular-DA conjugates were investigated and the relations describing the release of the neurotransmitters from both highly and poorly soluble conjugates are proposed by the authors (Juriga et al., 2018). In particular, it has been found that the release of neurotransmitter from poorly soluble polymer-DA conjugates such as **1** and **2** can be appropriately described considering the diffusion of DA from the solid surface into the solution coupled with the cleavage reactions occurring when the neurotransmitter is in solution (Juriga et al., 2018). The diffusion contribution may be expressed by the Higuchi equation (*i.e.*, $C_T = K_H \times t^{1/2}$) and that of the cleavage reactions may be described by a first order reaction rate. The overall reaction rate is given by a complex equation which for long times reaches a saturation value while for very short time or very slow cleavage reactions it can be converted to Higuchi equation (Juriga et al., 2018). Using such approach the measured percentages di DA released in FBS from conjugates **1** and **2** were plotted against the time or the square root of the time (Figure 4c and 4d) and the corresponding Higuchi parameters, useful for comparative kinetic purposes between the two conjugates, are shown in Table 1.

[Insert Figure 4 and Table 1]

From these results it is evident the higher stability of the amide conjugate **2** ($K_H$ values expressed as % x $h^{-1//2}$) compared to the ester one **1** ($K_H$ values expressed as % x $min^{-1//2}$) as well as that the former can allow prolonged neurotransmitter release.

### *3.4. Oxidative stability of conjugates **1** and **2***

To gain insight into the stability of DA towards autoxidation reaction when it is involved in polymeric conjugation with *N,O*-CMCS, the behavior of both ester **1** and amide **2** was studied under the stressed conditions described in Section 2.7., resembling one previously described by us (Cassano et al., 2020), but also adopting two new protocols. More precisely, in a first set of experiments, the time course of absorbances at 450 nm was monitored up to 24 h, after dispersion of the conjugates in a mixture composed of hydrogen peroxide (3%, v:v, 10 volumes stabilized):DMSO:water in 1:3:6 volume ratio, respectively, and the corresponding results are reported in Figure 5a. As shown, starting from about 4 h after dissolution in the mentioned ternary mixture, the solution of the neurotransmitter DA displayed intense absorbance at 450 nm attributable to the aminochrome (AC) (Bisaglia et al., 2007), so evidencing that the spontaneous autoxidation of DA is in progress (Figure 5a). In contrast, for ester **1** and amide **2**, only

**Table 1.** Experimental Higuchi parameters ($K_H$) in FBS for neurotransmitter release from the poorly soluble conjugates **1** and **2**

| **Conjugate** | **$K_H$** (FBS) |
|---|---|
| **1** | 2.477 ± 0.0 (% of DA released x $min^{-1//2}$) |
| **2** | 0.3776 ± 0.1258 (% of DA released x $h^{-1//2}$) |

few amounts of AC were evidenced starting from 17 h, indicating the suitability of both conjugates to be resistant to oxidative stress (Figure 5a). Such results were fully consistent with the experiments based on the exposure of the samples to air bubbling combined with the treatment of a dilute solution of hydrogen peroxide (3%, v/v) without freeze-drying treatment of the samples (Figure 5b). As it can be seen, in these experiments the absorbance at 282 nm (attributable to pure DA, according to (Bisaglia et al., 2007) is low and, particularly at the first time points, marked variations were noted for the control DA solution, while for pure *N,O*-CMCS and amide conjugate **2** such absorbance is higher and no significant changes over the time occur, confirming that conjugate **2** possess more stability towards autoxidation reaction. For a better evaluation of the stability profile towards the autoxidation reaction of conjugate **2**, the time course of absorbances at 386 and 450 nm were also monitored up to 24 h in PBS-pH 7.7 and the results are shown in Figure 5c.

[Insert Scheme 2 and Figure 5]

As for the DA autoxidation, it is reported that this reaction is controlled under acidic conditions but not in physiological/alkaline media where it is very fast (Umek et al., 2018). By monitoring UV bands at the wavelengths of 386 and 450 nm, AC could be detected according to the literature (Klegeris et al., 1995; Umek et al., 2018). As shown in Figure 5c, negligible amounts of such intermediate were detected at both wavelengths after exposure of conjugate **2** in comparison to free DA and its amount did not increase over time. Despite the fast autoxidation of DA, for amide conjugate **2** at both wavelengths the reduction of absorbance was in the range of 2-7 times less than the corresponding values of pure neurotransmitter (Figure 5c), proving the remarkable stability of *N,O*-Carboxymethyl Chitosan-DA amide conjugate **2**. In this experiment, pure *N,O*-CMCS was used as control. We have also investigated whether pure *N,O*-CMCS could contribute to the oxidation at 386 and 450 nm and

for the former wavelength acquired absorbances were around 10 times less than the ones of DA, whereas for the latter, negligible effect could be ascribed to the polymer due to the negative absorbances values.

### *3.5. MTT assay*

The biocompatibility of the amide conjugate **2** with OECs was assessed by the MTT assay. As shown in Figure 6a, the cytotoxicity was negligible when tested in a wide range of concentrations (from 0.3 to 75 μM). The low decrease in cell viability (6-8%) was similar to that determined by DMSO (6%) and parallels the same results previously obtained with the ester conjugate **1** (Cassano et al., 2020).

### *3.6. Uptake studies*

For uptake studies fluorescent amide conjugate **2** was obtained by covalent linkage of FITC (labelling efficiency of 100 μg FITC/mg FITC-CMCS-DA amide conjugate **2**). We tested in this assay the conjugate polymers bearing the highest DA concentrations that were also biocompatible with these cells, i.e. 18.75 and 75 μM. The uptake, measured by the percentage of positive cells, significantly increased with 75 μM DA at 2 h as compared with the lower concentration (Figure 6b). Interestingly, while the uptake also increased with 18.75 μM at 24 h as compared to 2 h, no further increase was obtained with 75 μM (Figure 6b). On the other hand, the mean fluorescent intensity (MFI), a measure of the average fluorescent in the overall population, corresponded well for 18.75 μM DA to the cell percentage, but also increased for the highest concentration (Figure 6c), differently from the cell percentage results (Figure 6b). Overall, these results indicate that while the percentage of cells internalizing the conjugate was already high at 2 h and reached a plateau, the internalization continued during time.

[Insert Figure 6]

## 4. Discussion

In the context of a research project aimed to develop polymer-DA conjugates potentially useful for nose-to-brain delivery of the neurotransmitter in a prolonged manner as a possible novel approach for the treatment of PD, we prepared, characterized and assessed the toxicity, uptake from olfactory bulb-derived cells of some *N*,*O*-CMCS-DA conjugates. In these polymer-conjugates, the catechol groups or the $–NH_2$ one of DA are covalently bound with

the –COOH groups of the polymer *N,O*-CMCS leading to conjugates among which the previously studied ester **1** (Cassano et al., 2020) and the currently investigated amide **2** evidenced interesting features. In order to find the best candidate for *in vivo* evaluations, in this work a comparative study between the delivery performances of amide **2** and those of ester **1** was carried out and the obtained results are discussed even from this point of view.

Comparing the synthetic approaches used for the preparation of ester conjugates previously studied (Cassano et al., 2020) with that described in this paper for amide **2**, it is evident that the preparative procedure used for obtaining the amide conjugate is much more direct and advantageous than those allowing the ester conjugates (Cassano et al., 2020). This is due to the necessary protection reactions of the appropriate functional groups of DA to prepare the ester conjugates and these reactions limit the overall yields of these last conjugates. In contrast, this limitation does not occur in the synthesis of amide conjugate **2** since there is not the need to protect the functional groups of DA.

In view of nasal administration, mucoadhesive properties of amide conjugate **2** compared to those of ester **1** were evaluated in SNF taking into account that once polymer/mucin interactions occurs, an increase in the residence time in the nasal cavity takes place (Ivarsson and Wahlgren, 2012). In this context, it should be considered that, among the polymer structural features, the presence of strong hydrogen bonding groups, high molecular weight and suitable chain flexibility increase the mucoadhesive properties (Palazzo et al., 2017). For chitosan-catechol containing conjugates, literature reports suggest that the presence of catechol moiety in the chain backbone of chitosan improves the mucoadhesive properties (Cassano et al., 2020; Kim et al., 2015; Ryu et al., 2015). These results from intermolecular associations between the catechol group grafted on CS and mucin in the contact step of the mucoadhesion process followed by the formation of covalent bonds mediated by catechol moiety in the next consolidation step (Kim et al., 2015; Ryu et al., 2015). On this basis, mucoadhesive properties for the conjugate **2** higher than ester **1** were expected. The observed comparable mucoadhesive properties of conjugates **1** and **2** suggest that, likely, the intermolecular associations catechol group/mucin are similar enough to those of (mono)esterified catechol group/mucin of **1** after 24 h of incubation. However, as above mentioned, it should be also considered that, during this period, both in SNF and in FBS hydrolytic cleavage of ester **1** may occur and it limits the application of this conjugate, as compared to **2**, for nose-to-brain delivery of the neurotransmitter DA. From data reported in Figure 4a and 4b, indeed, it is evident both the higher stability of conjugate **2** in SNF compared to **1** and the sustained neurotransmitter release from the former conjugate. Comparing the

Higuchi parameters ($K_H$ values) of the poorly soluble conjugates **1** and **2** (Table 1) in FBS, it is evident a faster neurotransmitter release from the former conjugate. It can be due to the easier hydrolytic cleavage of the ester function compared to the amide one as well as to the ubiquitous presence in the human body of esterase enzymes in comparison with the amidases. These results indicate that a much more prolonged release of DA can be obtained using the conjugate **2** and it is consistent with that observed for other polymer-DA amide conjugates (Juriga et al., 2018). Delivery systems allowing sustained release of the neurotransmitter as those based on conjugate **2** may be useful not only to avoid multiple administrations of DA (L-Dopa) but also to reduce the mentioned toxic effects emerging at later stages of the disease. Hence, they may represent an innovative approach to establish a disease modifying therapy of PD (Oertel and Schulz, 2016; Rodriguez-Nogales et al., 2016).

A further interesting result of this study is the observed oxidative stability of both conjugates **1** and **2** with the latter at a higher extent than the former (Figure 5). In details, we tested either oxidative stressed conditions in the presence of hydrogen peroxide or hydrogen peroxide/DMSO-free conditions, where the driving force for oxidation was represented by the pH value *(i.e.,* 7.7) of PBS, a more biomimetic medium (Umek et al., 2018). In our opinion, the observed stability to autoxidation reaction of conjugate **1** should be, in part, due to a hampered formation of *o*-quinone since one of the catechol hydroxyl groups is esterified (Scheme 2). In the case of **2**, the intramolecular Michael addition reaction leading to leucoaminochrome and then AC formation (Scheme 2) is not facilitated for the lower nucleophilic character of the nitrogen atom of the amido group present in the neurotransmitter moiety of this polymer conjugate.

Based on the higher stability to autoxidation reaction of conjugate **2** than conjugate **1**, it should be deduced that, likely, the structural limitation mentioned for the amide **2** is more severe than that proposed for ester **1**. Moreover, the negligible quantities of AC detected after 17 h incubation time of conjugates **1** and **2** (Figure 5a) could be probably due to the autoxidation of little amounts of *i*) free DA unreacted during the preparative synthetic method of conjugates and/or *ii*) the neurotransmitter possibly produced by hydrolytic cleavage of these conjugates. Moreover, it cannot be ruled out that, at longer incubation times, little amounts of further side reaction products could occur such as the oxidation of the free carboxylic acid groups of starting polymer *N,O*-CMCS leading to the formation of organic peracids. Overall, the higher stability towards the autoxidation reaction of **2** after 17 h of incubation constitutes a further advantage of this conjugate since it is expected to cause lower toxicity than that induced by L-Dopa. It is well known that, indeed, oxidative stress plays an important role in neurodegenerative diseases as PD and mitochondrial dysfunctions has been involved in this regard (Rodriguez-Nogales et al., 2016). Thus, generation in the mitochondria of ROS and free radicals as

well as the increase of DA metabolites from neurotransmitter autoxidation can be related to the chemical damage of dopaminergic cells (Oertel and Schulz, 2016; Rodriguez-Nogales et al., 2016).

The interesting profile of the amide conjugate **2** concerning release control and limited DA autoxidation is completed by its biocompatibility with OECs, *i.e.* those cells lining the olfactory nerve during its course from the olfactory mucosa to the olfactory bulb (Agrawal et al., 2018). Not only this, but also the higher internalization exerted by this amide conjugate of carboxymetyl chitosan in comparison with the ester conjugate (almost 80% vs. ~30%, as shown in (Cassano et al., 2020)) is indicating an efficiency profile useful for delivering DA to the brain nuclei involved in PD in a safe way. This internalization rate would be of crucial importance in delivering the DA-amide conjugate to the nasal cavity in a nose-to-brain approach. Indeed, the internalization by OECs was already high at 2 h of incubation. Considering that the $t_{1/2}$ mucociliary clearance in the nasal cavity is 20 min in humans (Sonvico et al., 2018), it may be possible that mucoadhesive properties of the amide conjugate **2** allow to increase residence time and internalization by olfactory nerve terminations (Ganger and Schindowski, 2018; Sonvico et al., 2018). From this standpoint, the controlled release of only 5-10% DA in the first days would benefit its nose-to-brain delivery. Moreover, the amounts of DA that we used in the uptake assay (2.9-11.5 μg/mL corresponding to 18.75-75 μM, see Fig. 6) appear to be clinically relevant because within the pharmacological range. In fact, in a recent study, Tang et al. (Tang et al., 2019) showed that DA-carrying nanoparticles was effective in alleviating motor symptoms in a rat model of PD at the dose of ~7.4 μg/mL), when administered intranasally. Finally, based on the DS value (560 μg of DA/ mg) of the amide conjugate **2**, it appears certainly possible, with appropriate dilutions, to prepare and administer intranasally to laboratory animals higher dosages of DA than those used in our vitro uptake assay, increasing the probability to reach effective concentrations of this neurotransmitter in the brain.

## 5. Conclusions

In this work, investigations concerning the conjugation of DA via ester or amide bond to *N,O*-CMCS were conducted. The higher stability of amide conjugate **2** was evidenced in terms of slow release in SNF without enzymes, in FBS and, importantly, in terms of protection from early DA oxidation, biocompatibility and high internalization by OECs. Further *in vivo* studies evaluating the profile performances of DA-conjugate **2** (and nanoparticles obtained by such conjugate) are planned to establish the clinical utility for PD treatment via the intranasal route of administration.

**Acknowledgements**

This work was partially financed by University of Bari (Italy) to A.T. (Cod. CUP:H91J11000160001).

595 **Declaration of competing interests:** The authors declare that they have no known competing financial interests or personal relationships that could have appeared to influence the work reported in this paper.

## REFERENCES


Agrawal, M., Saraf, S., Saraf, S., Antimisiaris, S.G., Chougule, M.B., Shoyele, S.A., Alexander, A., 2018. Nose-to-brain drug delivery: An update on clinical challenges and progress towards approval of anti-Alzheimer drugs. J Control Release 281, 139-177.

Ancona, A., Sportelli, M., Trapani, A., Picca, R.A., Palazzo, C., Bonerba, E., Mezzapesa, F., Tantillo, G., Trapani, G., Cioffi, N., 2014. Synthesis and Characterization of Hybrid Copper-Chitosan Nano-antimicrobials by Femtosecond Laser-Ablation in Liquids. Material Letters 136, 397-400.

Bisaglia, M., Mammi, S., Bubacco, L., 2007. Kinetic and structural analysis of the early oxidation products of dopamine: analysis of the interactions with alpha-synuclein. J Biol Chem 282, 15597-15605.

Bourganis, V., Kammona, O., Alexopoulos, A., Kiparissides, C., 2018. Recent advances in carrier mediated nose-to-brain delivery of pharmaceutics. Eur J Pharm Biopharm 128, 337-362.

Bukzem, A.L., Signini, R., Dos Santos, D.M., Liao, L.M., Ascheri, D.P., 2016. Optimization of carboxymethyl chitosan synthesis using response surface methodology and desirability function. Int J Biol Macromol 85, 615-624.

Cassano, R., Trapani, A., Di Gioia, M.L., Mandracchia, D., Pellitteri, R., Tripodo, G., Trombino, S., Di Gioia, S., Conese, M., 2020. Synthesis and characterization of novel chitosan-dopamine or chitosan-tyrosine conjugates for potential nose-to-brain delivery. Int J Pharm 589, 119829.

Cassano, R., Trombino, S., Bloise, E., Muzzalupo, R., Iemma, F., Chidichimo, G., Picci, N., 2007. New broom fiber (Spartium junceum L.) derivatives: preparation and characterization. J Agric Food Chem 55, 9489-9495.

Castellani, S., Trapani, A., Spagnoletta, A., di Toma, L., Magrone, T., Di Gioia, S., Mandracchia, D., Trapani, G., Jirillo, E., Conese, M., 2018. Nanoparticle delivery of grape seed-derived proanthocyanidins to airway epithelial cells dampens oxidative stress and inflammation. J Transl Med 16, 140.

Conese, M., Cassano, R., Gavini, E., Trapani, G., Rassu, G., Sanna, E., Di Gioia, S., Trapani, A., 2019. Harnessing Stem Cells and Neurotrophic Factors with Novel Technologies in the Treatment of Parkinson's Disease. Curr Stem Cell Res Ther 14, 549-569.

De Giglio, E., Trapani, A., Cafagna, D., Sabbatini, L., Cometa, S., 2011. Dopamine-loaded chitosan nanoparticles: formulation and analytical characterization. Anal Bioanal Chem 400, 1997-2002.

Denora, N., Cassano, T., Laquintana, V., Lopalco, A., Trapani, A., Cimmino, C.S., Laconca, L., Giuffrida, A., Trapani, G., 2012. Novel codrugs with GABAergic activity for dopamine delivery in the brain. Int J Pharm 437, 221-231.

Di Gioia, S., Trapani, A., Mandracchia, D., De Giglio, E., Cometa, S., Mangini, V., Arnesano, F., Belgiovine, G., Castellani, S., Pace, L., Lavecchia, M.A., Trapani, G., Conese, M., Puglisi, G., Cassano, T., 2015. Intranasal delivery of dopamine to the striatum using glycol chitosan/sulfobutylether-beta-cyclodextrin based nanoparticles. Eur J Pharm Biopharm 94, 180-193.

Ekladious, I., Colson, Y.L., Grinstaff, M.W., 2019. Polymer-drug conjugate therapeutics: advances, insights and prospects. Nat Rev Drug Discov 18, 273-294.

Ganger, S., Schindowski, K., 2018. Tailoring Formulations for Intranasal Nose-to-Brain Delivery: A Review on Architecture, Physico-Chemical Characteristics and Mucociliary Clearance of the Nasal Olfactory Mucosa. Pharmaceutics 10 (3), 116.

Hawthorne, G.H., Bernuci, M.P., Bortolanza, M., Tumas, V., Issy, A.C., Del-Bel, E., 2016. Nanomedicine to Overcome Current Parkinson's Treatment Liabilities: A Systematic Review. Neurotox Res 30, 715-729.

Ivarsson, D., Wahlgren, M., 2012. Comparison of in vitro methods of measuring mucoadhesion: ellipsometry, tensile strength and rheological measurements. Colloids Surf B Biointerfaces 92, 353-359.

Juriga, D., Laszlo, I., Ludanyi, K., Klebovich, I., Chae, C.H., Zrinyi, M., 2018. Kinetics of dopamine release from poly(aspartamide)-based prodrugs. Acta Biomater 76, 225-238.

Kaur, G., Arora, M., Ravi Kumar, M.N.V., 2019. Oral Drug Delivery Technologies-A Decade of Developments. J Pharmacol Exp Ther 370, 529-543.

Kim, K., Kim, K., Ryu, J.H., Lee, H., 2015. Chitosan-catechol: a polymer with long-lasting mucoadhesive properties. Biomaterials 52, 161-170.

Klegeris, A., Korkina, L.G., Greenfield, S.A., 1995. Autoxidation of dopamine: a comparison of luminescent and spectrophotometric detection in basic solutions. Free Radic Biol Med 18, 215-222.
Kreuter, J., 2014. Drug delivery to the central nervous system by polymeric nanoparticles: what do we know? Adv Drug Deliv Rev 71, 2-14.
Li, X., Tsibouklis, J., Weng, T., Zhang, B., Yin, G., Feng, G., Cui, Y., Savina, I.N., Mikhalovska, L.I., Sandeman, S.R., Howel, C.A., Mikhalovsky, S.V., 2017. Nano carriers for drug transport across the blood-brain barrier. J Drug Target 25, 17-28.
Mandracchia, D., Rosato, A., Trapani, A., Chlapanidas, T., Montagner, I.M., Perteghella, S., Di Franco, C., Torre, M.L., Trapani, G., Tripodo, G., 2017. Design, synthesis and evaluation of biotin decorated inulin-based polymeric micelles as long-circulating nanocarriers for targeted drug delivery. Nanomedicine 13, 1245-1254.
Mandracchia, D., Trapani, A., Perteghella, S., Sorrenti, M., Catenacci, L., Torre, M.L., Trapani, G., Tripodo, G., 2018. pH-sensitive inulin-based nanomicelles for intestinal site-specific and controlled release of celecoxib. Carbohydr Polym 181, 570-578.
Md, S., Khan, R.A., Mustafa, G., Chuttani, K., Baboota, S., Sahni, J.K., Ali, J., 2013. Bromocriptine loaded chitosan nanoparticles intended for direct nose to brain delivery: pharmacodynamic, pharmacokinetic and scintigraphy study in mice model. Eur J Pharm Sci 48, 393-405.
Mourya, V., K, , Inamdar, N.N., Tiwari, A., 2010. Carboxymethyl chitosan and its applications. Adv Mat Lett 1, 11-33.
Musani, I.E., Chandan, N.V., 2015. A comparison of the sedative effect of oral versus nasal midazolam combined with nitrous oxide in uncooperative children. Eur Arch Paediatr Dent 16, 417-424.
Musumeci, T., Pellitteri, R., Spatuzza, M., Puglisi, G., 2014. Nose-to-brain delivery: evaluation of polymeric nanoparticles on olfactory ensheathing cells uptake. J Pharm Sci 103, 628-635.
Oertel, W., Schulz, J.B., 2016. Current and experimental treatments of Parkinson disease: A guide for neuroscientists. J Neurochem 139 Suppl 1, 325-337.
Pagar, S.A., Shinkar, D.M., Saudagar, R.B., 2014. Development and evaluation of in situ nasal mucoadhesive gel of metoprolol succinate by using $3^2$ full factorial design. Int. J. Pharm. Pharm. Sci. 6, 218-223.
Pahuja, R., Seth, K., Shukla, A., Shukla, R.K., Bhatnagar, P., Chauhan, L.K., Saxena, P.N., Arun, J., Chaudhari, B.P., Patel, D.K., Singh, S.P., Shukla, R., Khanna, V.K., Kumar, P., Chaturvedi, R.K., Gupta, K.C., 2015. Trans-blood brain barrier delivery of dopamine-loaded nanoparticles reverses functional deficits in parkinsonian rats. ACS Nano 9, 4850-4871.
Palazzo, C., Trapani, G., Ponchel, G., Trapani, A., Vauthier, C., 2017. Mucoadhesive properties of low molecular weight chitosan- or glycol chitosan- and corresponding thiomer-coated poly(isobutylcyanoacrylate) core-shell nanoparticles. Eur J Pharm Biopharm 117, 315-323.
Patel, T., Zhou, J., Piepmeier, J.M., Saltzman, W.M., 2012. Polymeric nanoparticles for drug delivery to the central nervous system. Adv Drug Deliv Rev 64, 701-705.
Perteghella, S., Mandracchia, D., Torre, M.L., Tamma, R., Ribatti, D., Trapani, A., Tripodo, G., 2020. Anti-angiogenic activity of N,O-carboxymethyl-chitosan surface modified solid lipid nanoparticles for oral delivery of curcumin. J. Drug Deliv. Sci. Technol. 56, 101494.
Pillay, S., Pillay, V., Choonara, Y.E., Naidoo, D., Khan, R.A., du Toit, L.C., Ndesendo, V.M., Modi, G., Danckwerts, M.P., Iyuke, S.E., 2009. Design, biometric simulation and optimization of a nano-enabled scaffold device for enhanced delivery of dopamine to the brain. Int J Pharm 382, 277-290.
Rashed, E.R., Abd El-Rehim, H.A., El-Ghazaly, M.A., 2015. Potential efficacy of dopamine loaded-PVP/PAA nanogel in experimental models of Parkinsonism: possible disease modifying activity. J Biomed Mater Res A 103, 1713-1720.
Reeve, A., Simcox, E., Turnbull, D., 2014. Ageing and Parkinson's disease: why is advancing age the biggest risk factor? Ageing Res. Rev. 14, 19–30.
Rodriguez-Nogales, C., Garbayo, E., Carmona-Abellan, M.M., Luquin, M.R., Blanco-Prieto, M.J., 2016. Brain aging and Parkinson's disease: New therapeutic approaches using drug delivery systems. Maturitas 84, 25-31.
Ryu, J.H., Hong, S., Lee, H., 2015. Bio-inspired adhesive catechol-conjugated chitosan for biomedical applications: A mini review. Acta Biomater 27, 101-115.

Samaridou, E., Alonso, M.J., 2018. Nose-to-brain peptide delivery - The potential of nanotechnology. Bioorg Med Chem 26, 2888-2905.

Saraiva, C., Praca, C., Ferreira, R., Santos, T., Ferreira, L., Bernardino, L., 2016. Nanoparticle-mediated brain drug delivery: Overcoming blood-brain barrier to treat neurodegenerative diseases. J Control Release 235, 34-47.

Singh, A., Kutscher, H.L., Bulmahn, J.C., Mahajan, S.D., He, G.S., Prasad, P.N., 2020. Laser ablation for pharmaceutical nanoformulations: Multi-drug nanoencapsulation and theranostics for HIV. Nanomedicine 25, 102172.

Sonvico, F., Clementino, A., Buttini, F., Colombo, G., Pescina, S., Staniscuaski Guterres, S., Raffin Pohlmann, A., Nicoli, S., 2018. Surface-Modified Nanocarriers for Nose-to-Brain Delivery: From Bioadhesion to Targeting. Pharmaceutics 10.

Tang, S., Wang, A., Yan, X., Chu, L., Yang, X., Song, Y., Sun, K., Yu, X., Liu, R., Wu, Z., Xue, P., 2019. Brain-targeted intranasal delivery of dopamine with borneol and lactoferrin co-modified nanoparticles for treating Parkinson's disease. Drug Deliv 26, 700-707.

Trapani, A., De Giglio, E., Cafagna, D., Denora, N., Agrimi, G., Cassano, T., Gaetani, S., Cuomo, V., Trapani, G., 2011. Characterization and evaluation of chitosan nanoparticles for dopamine brain delivery. Int J Pharm 419, 296-307.

Trapani, A., Mandracchia, D., Tripodo, G., Cometa, S., Cellamare, S., De Giglio, E., Klepetsanis, P., Antimisiaris, S.G., 2018. Protection of dopamine towards autoxidation reaction by encapsulation into non-coated- or chitosan- or thiolated chitosan-coated-liposomes. Colloids Surf B Biointerfaces 170, 11-19.

Trapani, A., Palazzo, C., Contino, M., Perrone, M.G., Cioffi, N., Ditaranto, N., Colabufo, N.A., Conese, M., Trapani, G., Puglisi, G., 2014. Mucoadhesive properties and interaction with P-glycoprotein (P-gp) of thiolated-chitosans and -glycol chitosans and corresponding parent polymers: a comparative study. Biomacromolecules 15, 882-893.

Trapani, G., Franco, M., Trapani, A., Lopedota, A., Latrofa, A., Gallucci, E., Micelli, S., Liso, G., 2004. Frog intestinal sac: a new in vitro method for the assessment of intestinal permeability. J Pharm Sci 93, 2909-2919.

Umek, N., Gersak, B., Vintar, N., Sostaric, M., Mavri, J., 2018. Dopamine Autoxidation Is Controlled by Acidic pH. Front Mol Neurosci 11, 467.

Wollmer, E., Klein, S., 2017. A review of patient-specific gastrointestinal parameters as a platform for developing in vitro models for predicting the in vivo performance of oral dosage forms in patients with Parkinson's disease. Int J Pharm 533, 298-314.

**Captions to Figures**

**Figure 1.** Chemical structures of ester and amide *N,O*-CMCS-DA conjugates **1** and **2**, respectively.

**Figure 2.** 1H-NMR spectrum of N,O-CMCS-DA amide conjugate **2**.

**Figure 3.** Mucoadhesive properties in SNF/DMSO of ester conjugate **1** (red), amide conjugate **2** (blue), parent *N,O*-CMCS polymer (yellow) and HEC (green) taken as positive control.

**Figure 4.** Cumulative DA released in SNF from amide conjugate **2** (a) and ester **1** (b) (Cassano et al., 2020). Dopamine released in FBS from the ester conjugate **1** (c) and corresponding square root dependency (d); dopamine released in FBS from the amide conjugate **2** (e) and corresponding square root dependency (f).

**Figure 5.** a) Time course of absorbance recorded at λ 450 nm after treatment of pure DA solution (blue) or conjugates **1** (red) and **2** (green) treated with a mixture of hydrogen peroxide:DMSO:water in 1:3:6 volume ratio, respectively; b) Variations of absorbance recorded at the wavelength of 282 nm after exposition of pure DA solution (blue) or pure *N,O*-CMCS (yellow) or conjugate **2** (green) to air bubbling for 1 min combined with a dilute solution of hydrogen peroxide (3% v/v) treatment recording the corresponding UV spectra at scheduled time intervals as well as at 48 h without freeze drying treatment of samples; c) Monitoring the absorbance values at the wavelength of 386 nm and 450 nm of pure DA (1 mM), pure *N,O*-CMCS or conjugate **2** (1 mM in DA) exposed in PBS 100 mM pH 7.6 without hydrogen peroxide and DMSO. Legend: control DA solution (light blue tone at λ = 386 nm, blue at λ = 450 nm); amide conjugate **2** (light green tone at λ = 386 nm, green at λ = 450 nm); pure *N,O*-CMCS (light yellow tone at λ = 386 nm, yellow at λ = 450 nm).

**Figure 6**. a) Cytotoxicity of the amide conjugate. OECs were challenged with the indicated concentrations of amide conjugate **2** for 24 h. Cells were then assayed for vitality by the MTT assay. Negative controls (NC) are untreated cells (100% of vitality), whereas DMSO denotes cells treated with 0.1% DMSO and TX-100 those treated with 10% Triton-X-100 (positive controls). ***$p<0.0001$ TX-100 vs all other conditions. Data are the results of two-three experiments each carried out in six wells. b) and c) Cellular uptake of FITC-CMCS-DA **2** by OECs. b) and c) show percentage of positive cells and mean fluorescent intensity (MFI), respectively. Data are the results of two experiments each carried in triplicate. In b) *$p>0.05$; in c) ***$p<0.0001$.

**Scheme 1.** The synthetic pathway followed to prepare *N,O,*-CMCS-DA amide conjugate **2**.

**Scheme 2.** The oxidative pathway of dopamine to form aminochrome.

**Figure S1.** a) FT-IR spectra of pure DA *i*), pure *N,O*-CMCS *ii*), amide conjugate **2** *iii*); b) DSC thermograms of pure DA *i*), pure *N,O*-CMCS *ii*), amide conjugate **2** *iii*).

Figure(s)

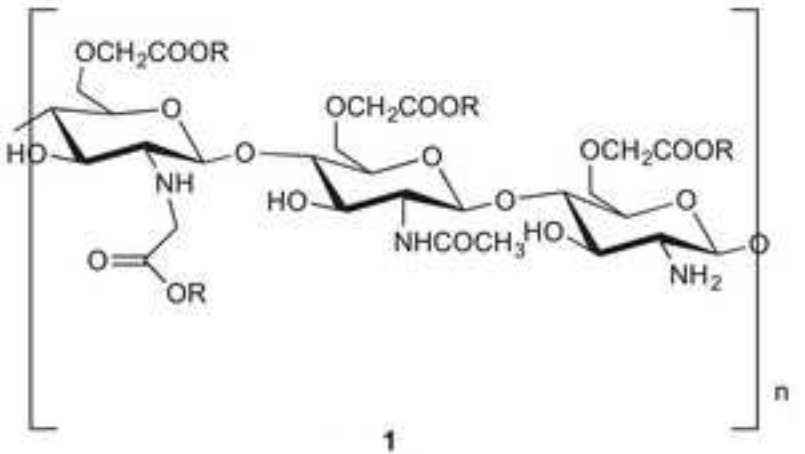


1

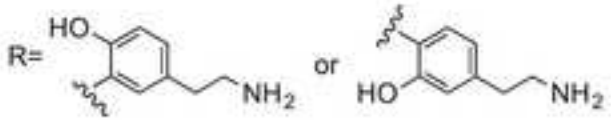


mixture of *m*- and *p*- isomers

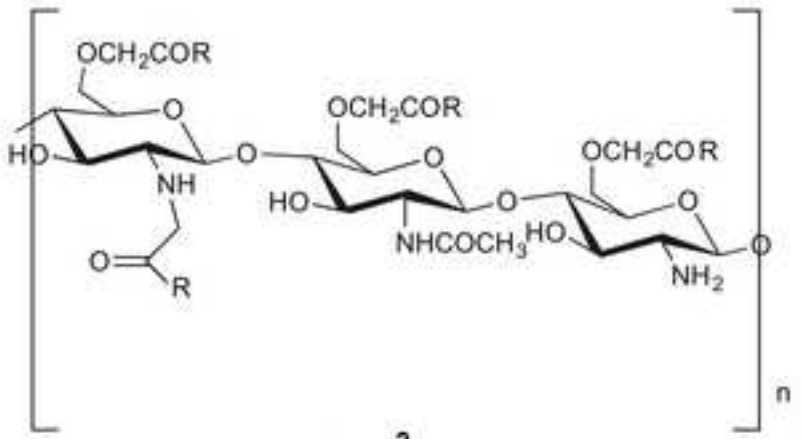


2

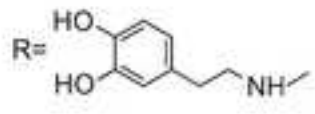

Figure(s)

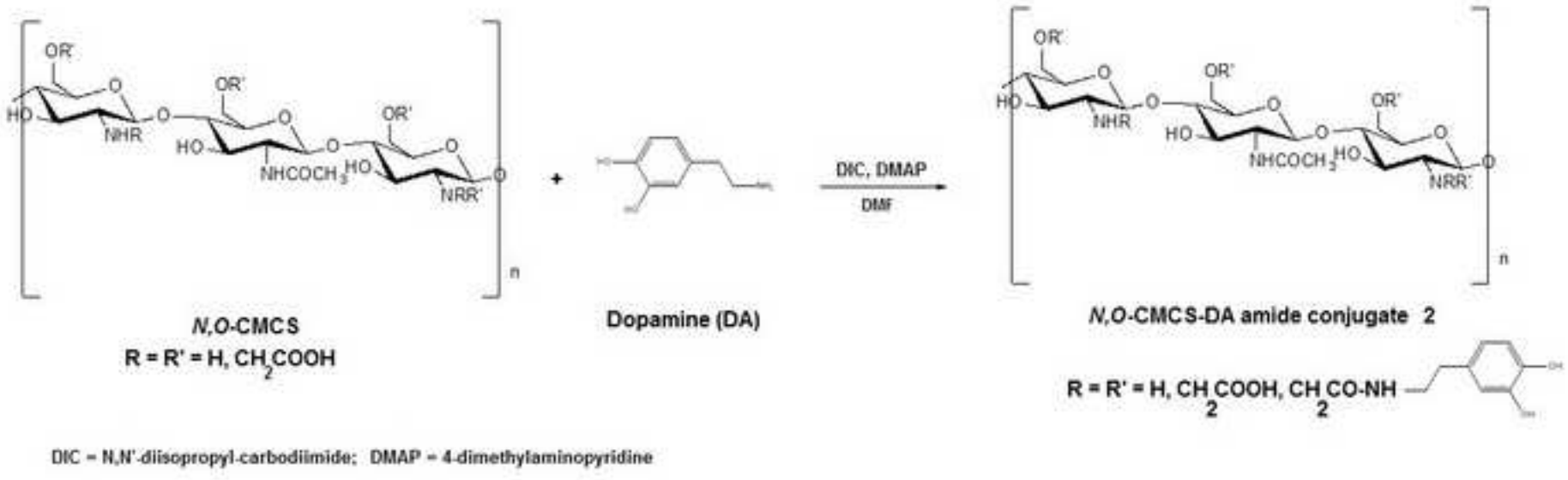


DIC = N,N'-diisopropyl-carbodiimide; DMAP = 4-dimethylaminopyridine

Figure(s)

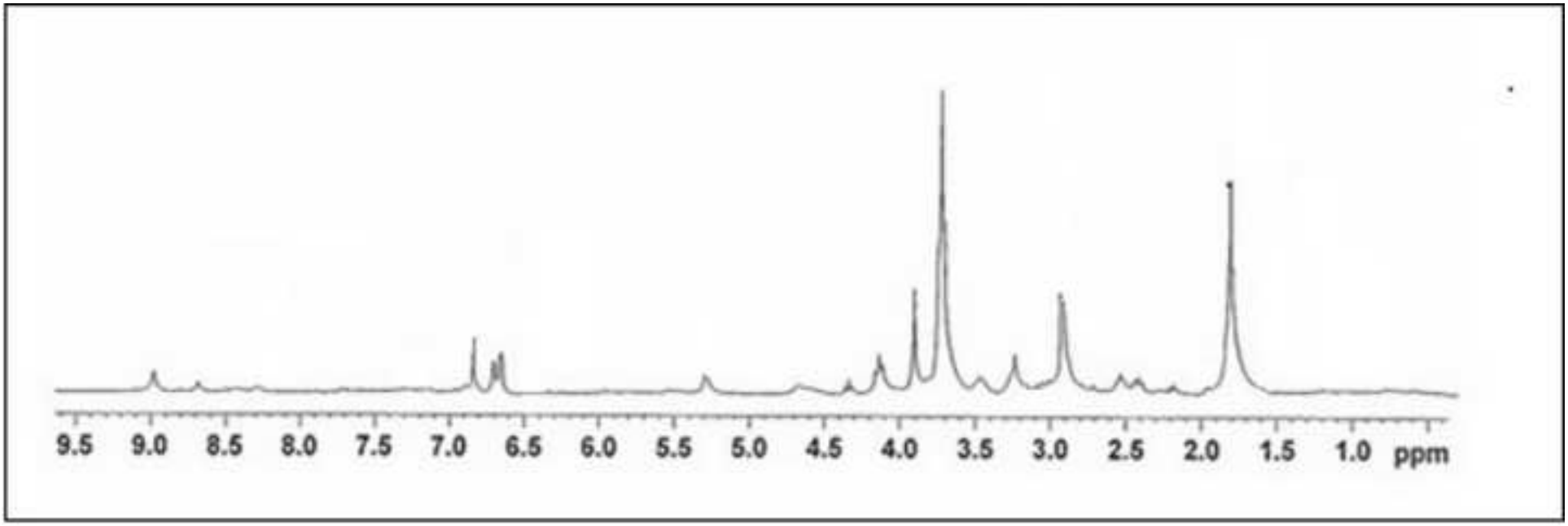

Figure(s)

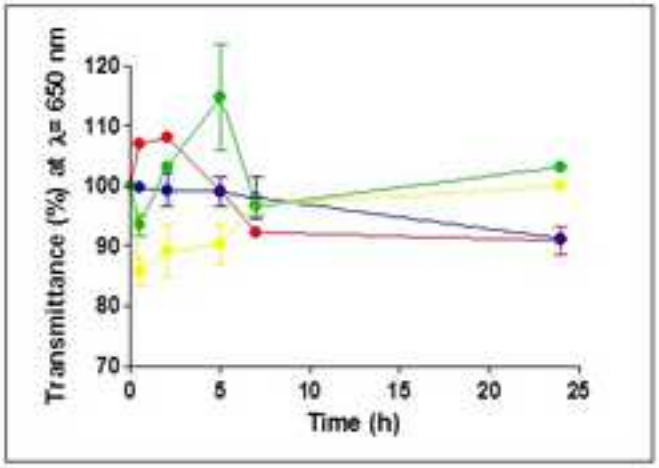
Transmittance (%) at λ= 650 nm
120
110
100
90
80
70
0
5
10
15
20
25
Time (h)

Figure(s)

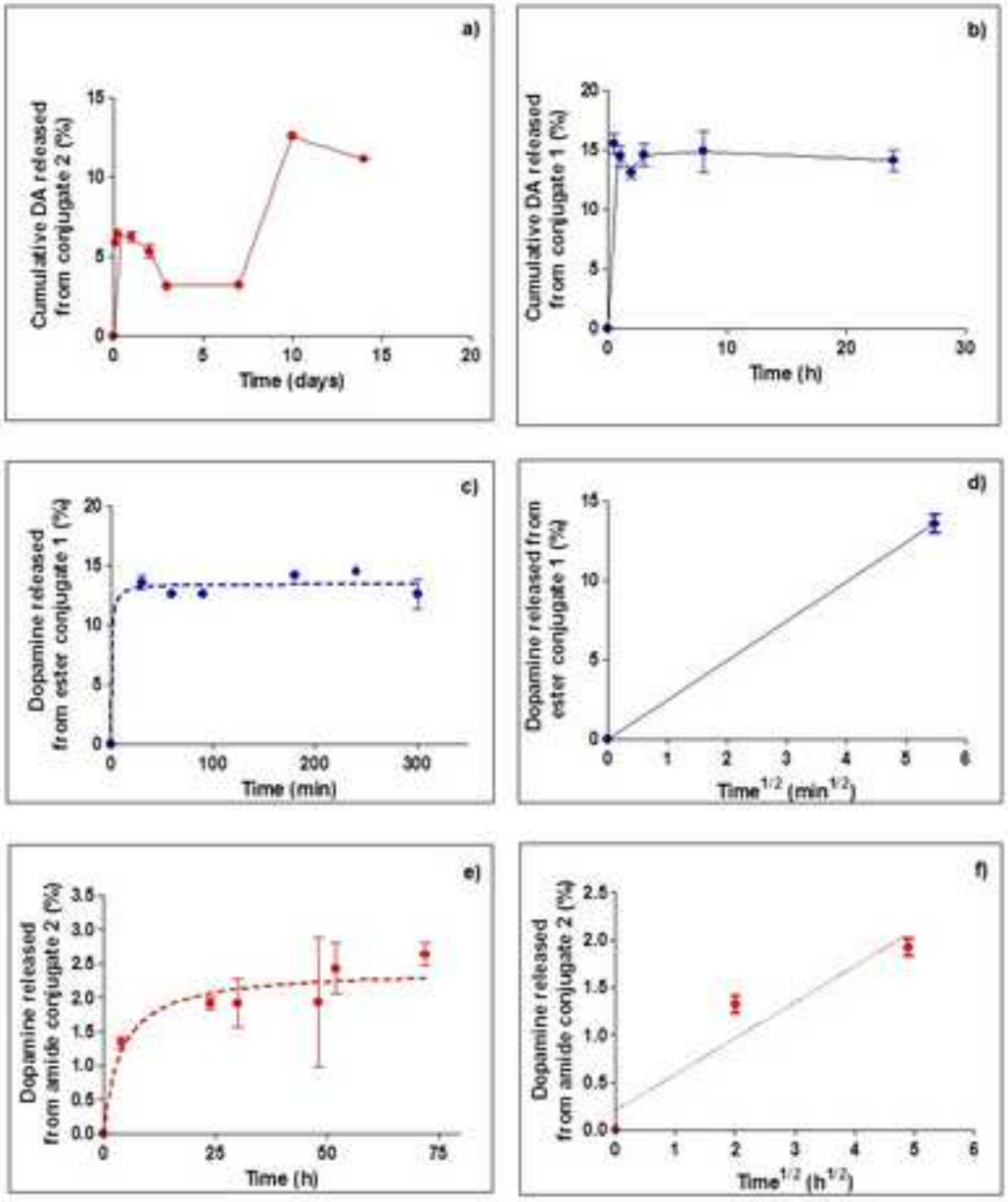
a)
Cumulative DA released from conjugate 2 (%)
Time (days)
b)
Cumulative DA released from conjugate 1 (%)
Time (h)
c)
Dopamine released from ester conjugate 1 (%)
Time (min)
d)
Dopamine released from ester conjugate 1 (%)
Time$^{1/2}$ (min$^{1/2}$)
e)
Dopamine released from amide conjugate 2 (%)
Time (h)
f)
Dopamine released from amide conjugate 2 (%)
Time$^{1/2}$ (h$^{1/2}$)

Figure(s)

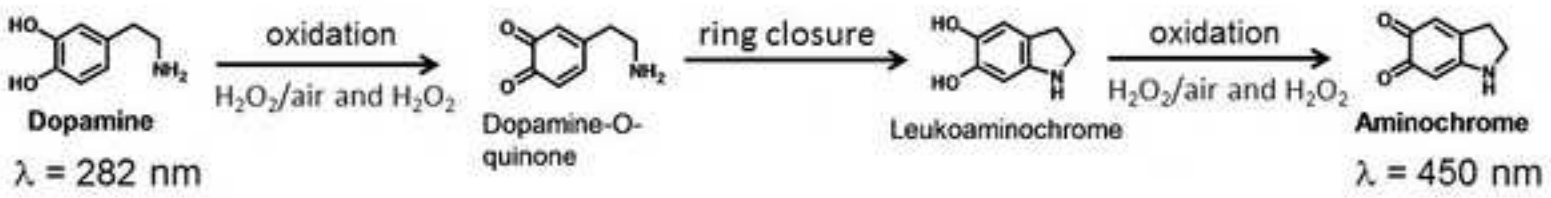
oxidation
$H_2O_2$/air and $H_2O_2$
ring closure
oxidation
$H_2O_2$/air and $H_2O_2$
Dopamine
λ = 282 nm
Dopamine-O-quinone
Leukoaminochrome
Aminochrome
λ = 450 nm

Figure(s)

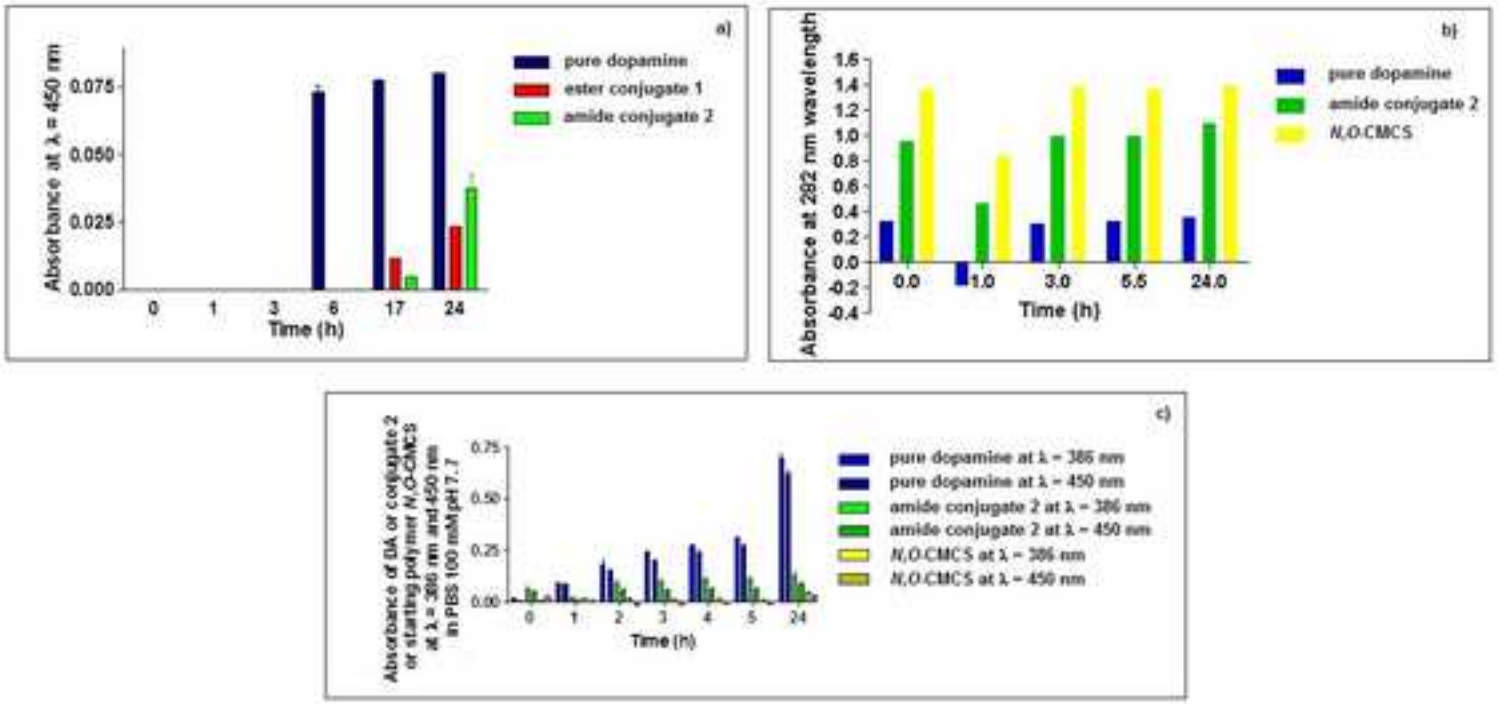
a)
Absorbance at λ = 450 nm
0.000
0.025
0.050
0.075
0
1
3
6
17
24
Time (h)
pure dopamine
ester conjugate 1
amide conjugate 2
b)
Absorbance at 292 nm wavelength
-0.4
-0.2
0.0
0.2
0.4
0.6
0.8
1.0
1.2
1.4
1.6
0.0
1.0
3.0
5.5
24.0
Time (h)
pure dopamine
amide conjugate 2
N,O-CMCS
c)
Absorbance of DA or conjugate 2 or starting polymer N,O-CMCS at λ = 386 nm and 450 nm in PBS 100 mM pH 7.7
0.00
0.25
0.50
0.75
0
1
2
3
4
5
24
Time (h)
pure dopamine at λ = 386 nm
pure dopamine at λ = 450 nm
amide conjugate 2 at λ = 386 nm
amide conjugate 2 at λ = 450 nm
N,O-CMCS at λ = 386 nm
N,O-CMCS at λ = 450 nm

Figure(s)

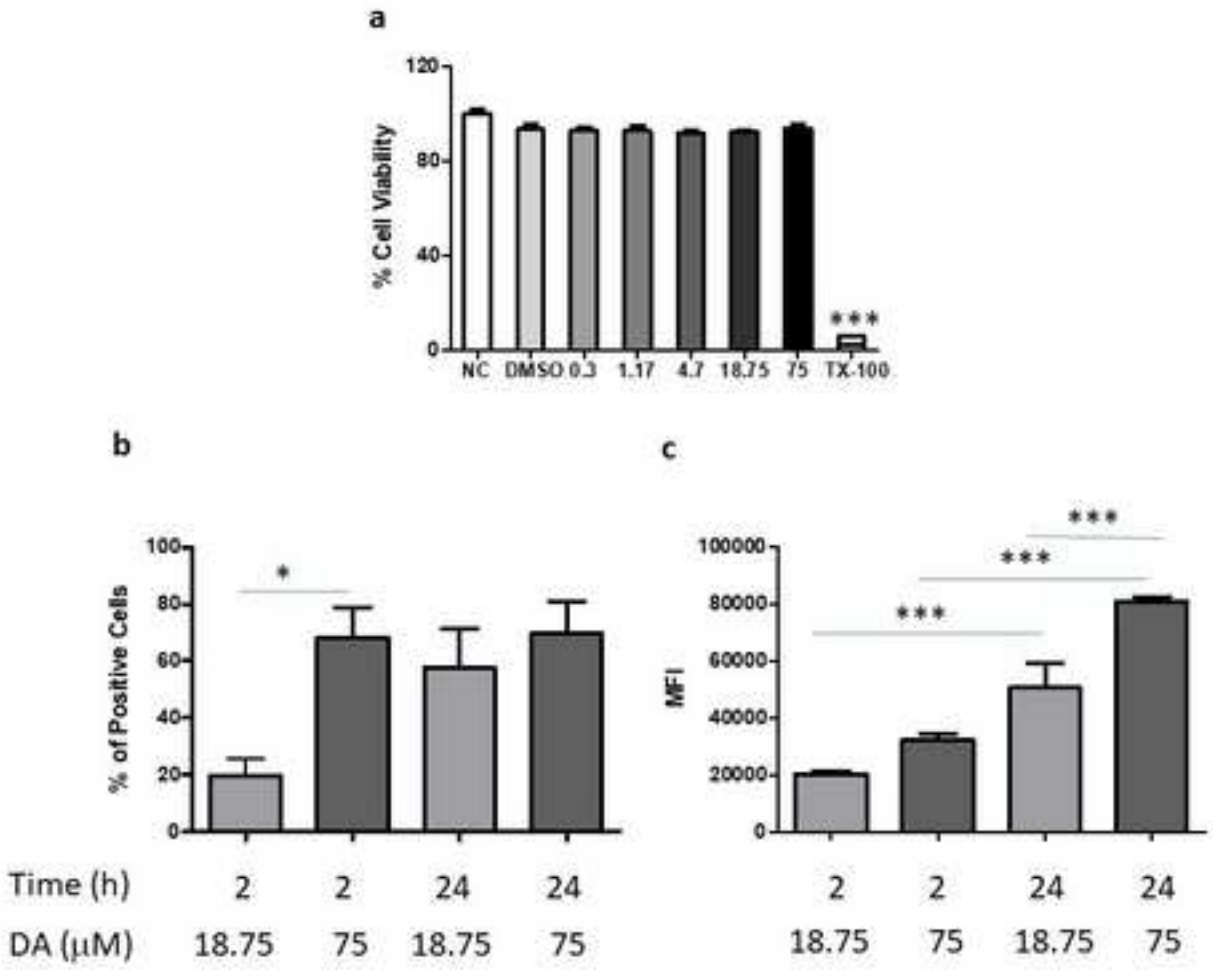
a
% Cell Viability
120
80
40
0
***
NC DMSO 0.3 1.17 4.7 18.75 75 TX-100
b
% of Positive Cells
100
80
60
40
20
0
*
c
MFI
100000
80000
60000
40000
20000
0
***
***
***
Time (h) 2 2 24 24
DA (μM) 18.75 75 18.75 75
2 2 24 24
18.75 75 18.75 75

Figure(s)

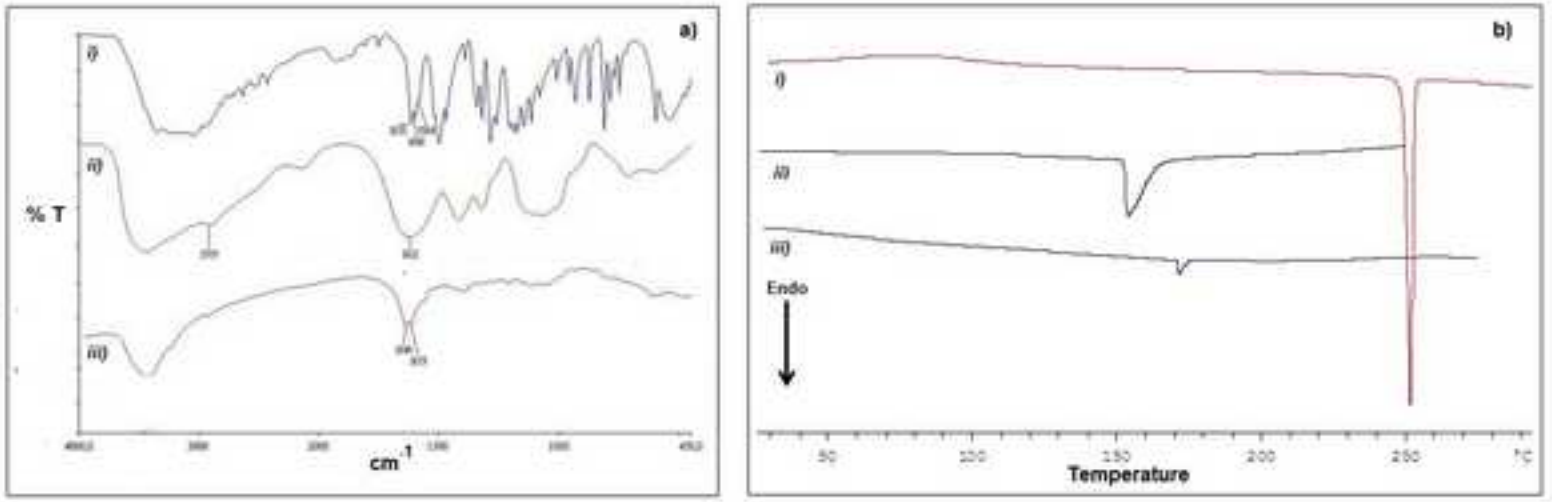

**Nose-to-brain delivery: a comparative study between carboxymethyl chitosan based conjugates of dopamine**

Sante Di Gioia[a], Adriana Trapani,[b*] Roberta Cassano,[c*] Saverio Cellamare,[b] Isabella Bolognino,[b] Maria Luisa Di Gioia,[c] Sonia Trombino,[c] Md Niamat Hossain[a], Enrico Sanna,[d] Giuseppe Trapani, [b] and Massimo Conese[a]

[a]*Department of Medical and Surgical Sciences, University of Foggia, 71122 Foggia, Italy*

[b]*Department of Pharmacy-Drug Sciences, University of Bari "Aldo Moro", 70125 Bari, Italy*

[c]*Department of Pharmacy, Health and Nutritional Sciences, University of Calabria, 87036 Arcavacata di Rende, Cosenza, Italy*

[d]*Department of Life and Environmental Sciences, Section of Neuroscience and Anthropology, University of Cagliari, Monserrato (Cagliari), Italy*

Sante Di Gioia: Data curation; Formal analysis; Investigation.

Adriana Trapani: Conceptualization; Project administration; Writing - review & editing; Supervision.

Roberta Cassano: Project administration; Roles/Writing - original draft.

Saverio Cellamare: Investigation; Software; Methodology.

Isabella Bolognino: Investigation; Data curation.

Maria Luisa Di Gioia: Funding acquisition; Methodology.

Sonia Trombino: Funding acquisition; Methodology.

Enrico Sanna: Validation; Visualization.

Giuseppe Trapani: Validation; Visualization.

Massimo Conese: Conceptualization; Validation; Methodology.